Supporting Information

Li et al. 10.1073/pnas.1300524110

SI Materials and Methods

Most derivatized crystals diffracted to between 5- and 7-Å resolution and the majority of native crystals diffracted to 4.0-Å resolution with exception of crystals soaked overnight in 5 mM $UO_2(acetate)_2$, which diffracted at up to 3.3-Å resolution with noticeable changes in unit cell dimensions and strongly detectable anomalous signal. Soaking of the uranium compound at concentrations of 0.5 mM or lower failed to induce the same changes in unit cell dimensions or to produce anomalous signal. This suggests that the uranium binding sites are weak and are involved in crystal packing. The typical unit cell dimensions for most native datasets including the best native crystal in space group *C2* at 3.27 Å resolution were $a = 137.4$ Å, $b = 56.2$ Å, $c = 94.9$ Å, and $\beta = 94.9°$. *C2* unit cell dimensions for U-soaked crystals were $a = 136.7$ Å, $b = 54.5$ Å, $c = 95.9$ Å, and $\beta = 92.2°$. With large changes in unit cell dimensions, isomorphous amplitude differences between U-soaked derivative and native datasets were in the range of 42–45%, suggesting that there was significant nonisomorphism. All crystals also suffered from severe anisotropy with B factors in principal axes different by more than 40 $Å^2$. The three U-soaked datasets differed from each other by 9%–13% at 3.5-Å resolution. By merging these three U datasets together, we greatly enhanced the anomalous signal, whereas ignoring subtle differences in their heavy atom structures. Only merged U-data single-anomalous scattering (SAS) phasing resulted in interpretable maps initially. Addition of back-soaked native data at 3.8-Å resolution during SAS phasing greatly increased the score of the correct solution relative to nonsolutions in Phenix, although the quality of the maps improved only slightly. The back-soaked native crystals were prepared by soaking 5 mM UO_2Ac_2 overnight followed by 30-s, 60-s, and 30-min soaks without UO_2Ac_2 followed by crystal freezing. Back soaking for 30 s removed nearly all bound U and reduced the diffraction to 3.8-Å resolution. Back soaking for 60 s or 30 min reduced the diffraction to 4.2- and 6-Å resolution, respectively.

Although single-isomorphous replacement (SIR) phases paired between each of the three U-soaked derivatives and each of the two back-soaked natives (30 s and 60 s) produced clear solvent boundaries, we were unable to include them in the final phasing procedures, partly because the corresponding native datasets had lower resolutions (3.8 and 4.2 Å) relative to the U datasets, and partly because the figures of merit were inflated such that their phases were not modified by the domain averaging procedure.

We assumed that the crystal packing in the original native and U-soaked crystal forms was similar despite large amplitude differences between them. Starting with identity matrices for each domain for the native structure, we included the unphased native structure as a second crystal in DMMULTI to define domain-orientation matrices. This procedure allowed us to transfer the best U-experimental phases to the native structure. With these phases, we were able to solve partially substituted SeMet substructures using isomorphous difference Fourier as well as anomalous difference Fourier methods. We had collected three SeMet datasets, one collected at Se peak wavelength (Se at 3.5-Å resolution), one at Hg-peak wavelength after soaking ethylmercurial phosphate into crystals (SeHg at 4.0-Å resolution), and one at Ta-peak wavelength after soaking Ta_6Br_{12} into crystals (SeTaBr at 4.0-Å resolution). Isomorphous differences between the S-Met native and each of the three SeMet derivative datasets were 20.2%, 17.2%, and 17.1%, respectively for Se, SeHg, and SeTaBr. Isomorphous differences between Se and SeHg, between Se and SeTaBr, and between SeHg and SeTaBr were 14.3%, 9.2%, and 11.8%, respectively. With externally phased heavy-atom structure refinement, we were able to accurately define Se substructures and calculate experimental phases using corresponding Se-S pairs. The experimental maps calculated using combined Se-S paired SIR phases for the native structure revealed a clear solvent boundary for each domain. Once these new phases were included in DMMULTI, the density-modified experimental maps were greatly improved in both the U-soaked structure and the native structure. After a systematic search for sharpened structures during density averaging and modification using DMMULTI, the best experimental maps were obtained when the amplitudes for both U-soaked structure and native were sharpened by $B = -20$ $Å^2$. Based on these experimental maps, we were able to trace the polypeptide chain, assign its sequence continuously from D783 through E1023, and identify one intersubunit and six intrasubunit disulfide bonds in addition to four N-linked glycans (on N809, N878, N922, and N990).

The structure was refined at 3.27-Å resolution with Phenix and Refmac, and rebuilt with Coot. Due to relatively low solvent content of 55%, there were ~2.66 observations to be refined per atom in the asymmetric unit. Refinement was carried out using strong experimental phase constraints and domain-related twofold non-crystallographic symmetry (NCS) restraints in initial cycles, with gradual removal of these constraints in the last few cycles.

The location of domain I in E2-ECD was initially identified in $F_o–F_c$ maps and $2F_o–F_c$ maps using the ΔN90-E2-ECD molecular replacement model, with a free R factor of 45%. The quality of maps for domain I was improved with iterative DMMULTI runs with experimental phases derived from the UO_2Ac_2 and native ΔN90-E2-ECD datasets. These phases were used as external constraints for the refinement (expressed as Hendrickson–Lattman coefficients). The best results for DMMULTI runs and refinement of E2-ECD were obtained when all data to 3.5-Å resolution were included after applying an anisotropic correction to the data followed by B-factor sharpening by a factor of −20 $Å^2$. Separated β strands were only visible in the electron density when the data up to 3.5-Å resolution were included.

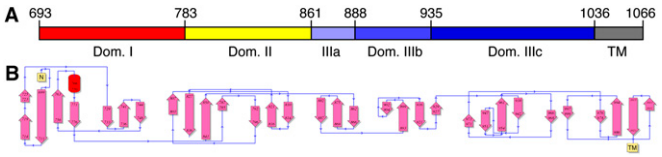

Fig. S1. Secondary structure topology of bovine viral diarrhea virus (BVDV) E2. (*A*) The three-domain topology of E2. Domain I is in red, domain II is in yellow, and domain III is in shades of blue: light blue for module IIIa, medium blue for module IIIb, and dark blue for module IIIc. Residue numbers follow BVDV polyprotein numbering. The transmembrane domain (gray) is missing in the structure. (*B*) Secondary structure topology diagram of BVDV E2 domains II and III generated with PDBsum Generate. Domain I was omitted from the analysis due to the poor quality of the electron density and lack of model atomic coordinates refined at high resolution for domain I.

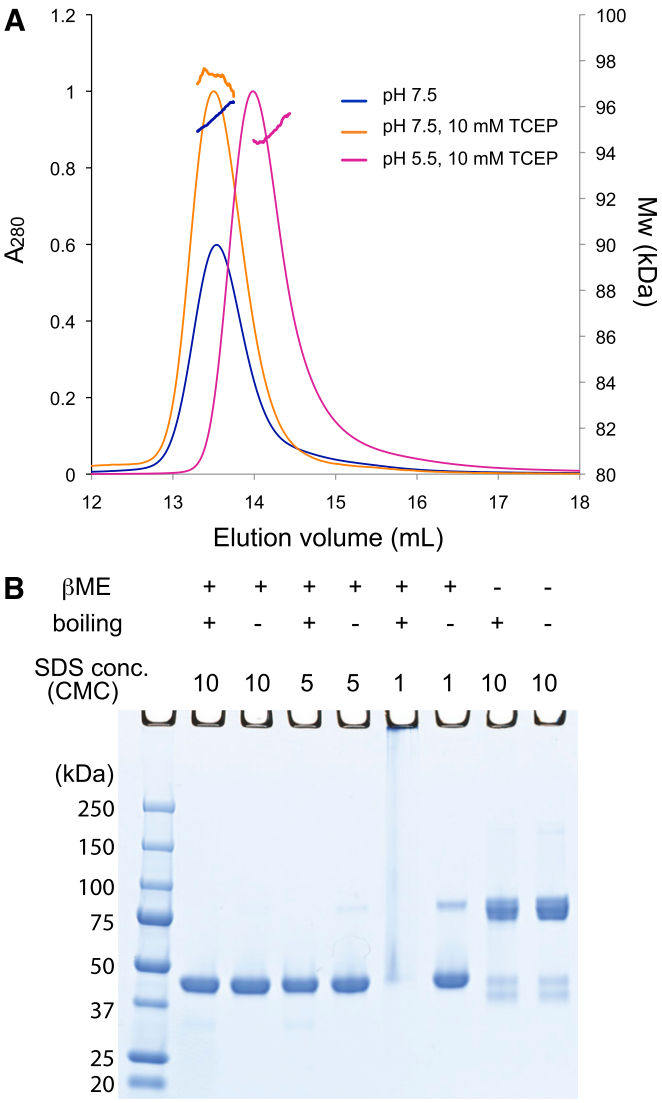

Fig. S2. BVDV E2 is a dimer in solution at different pH conditions. (*A*) The amount of 0.1 mL of E2 (1–3 g/L) was loaded onto a Superdex 200 30/100 size-exclusion column preequilibrated with different buffers: blue, 50 mM triethanolamine pH 7.5, 50 mM NaCl; orange, 50 mM triethanolamine pH 7.5, 50 mM NaCl, 10 mM TCEP; and magenta, 10 mM NaOAc pH 5.5, 50 mM NaCl, 10 mM Tris(2-carboxyethyl)phosphine. The eluate was analyzed for absorbance at 280 nm (*Left y* axis) and for multiangle light scattering, which was converted into molecular mass (*Right y* axis, see *Materials and Methods*). (*B*) SDS/PAGE of BVDV E2 under reducing conditions (0.31 M β-mercaptoethanol, βME) or nonreducing conditions, with or without heating of the sample before loading, and in the presence of various concentrations of SDS [0.1–1% (wt/vol)] in the loading buffer. E2 dimers dissociate under reducing conditions even without heating in the presence of SDS at concentrations above the critical micelle concentration [CMC, 0.1% (wt/vol)].

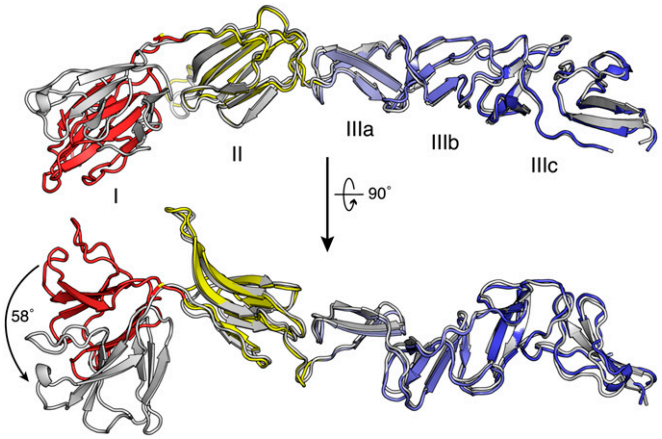

Fig. S3. Variable orientation of domain I relative to domain II. Comparison of the two subunits in the asymmetric unit of the full-length E2 ectodomain structure. Subunit A (gray) is shown in the same two orientations as in Fig. 1 *B* and *C*. Subunit B (in the same color scheme as subunit A in Fig. 1) is shown with domains II and III superimposed onto those of subunit A. The orientation of domain I relative to domain II differs by 58° in the two subunits.

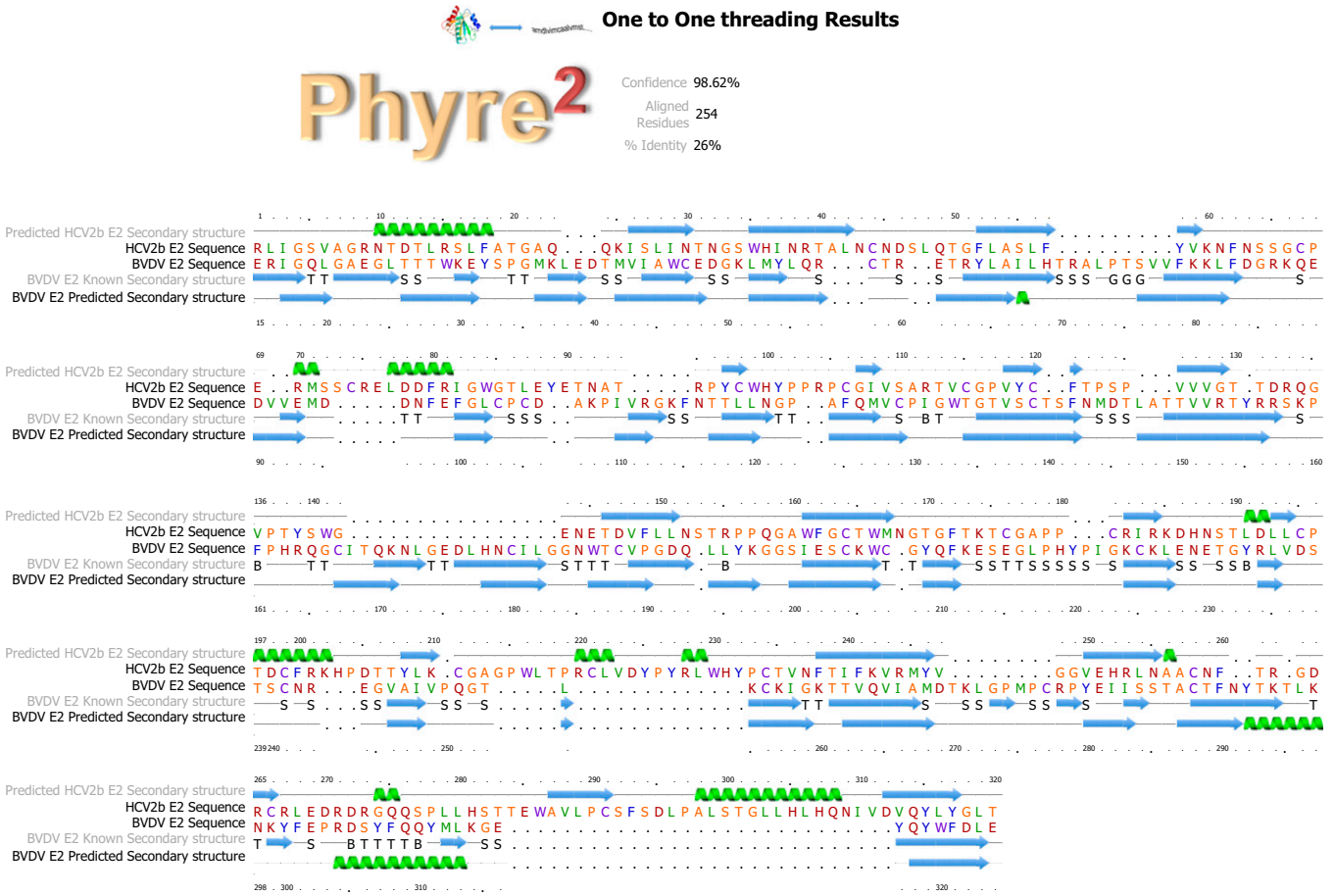

Fig. S4. Sequence alignment of the BVDV and hepatitis C virus (HCV)2b E2 sequences using secondary structure scoring. Global sequence alignment resulting from one-to-one threading of the HCV2b E2 sequence into the BVDV E2 structure with Phyre2. Phyre2 scores the fit of the predicted secondary structure of the query sequence (HCV2b) to the known secondary structure of the template structure (BVDV E2). The secondary structure weight was set to 0.9. The secondary structure of BVDV E2 is shown, along with the secondary structure of HCV2b E2 and BVDV E2 predicted from the respective amino acid sequences.

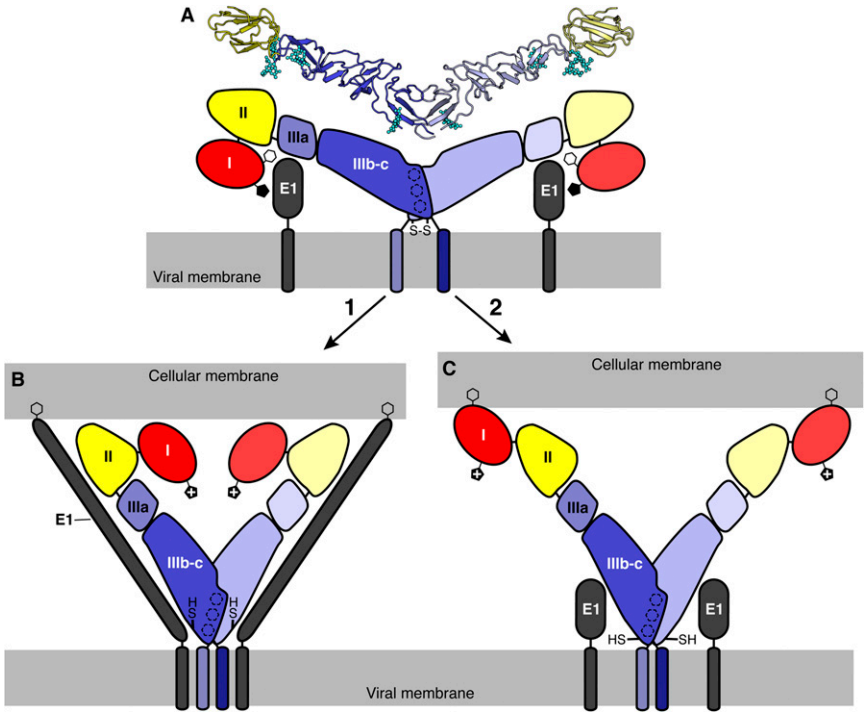

Fig. S5. Proposed fusion mechanisms if the E2 dimer is stable. Three alternative mechanisms are proposed for insertion of a fusion motif into the target host cell membrane with a stable E2 dimer as the functional unit. (*A*) E2 forms a disulfide-linked dimer and is associated with E1 on the surface of the infectious virion. The black pentagon represents the unprotonated side chain of His762. (*B*) E1 contains the fusion motif. E2 functions as a coeffector of fusion providing structural integrity to the fusion complex. Protonation of His762 controls exposure of the fusion motif in E1 by destabilizing an interaction between E2 and the fusion motif. (*C*) Domain I contains an as yet unidentified fusion motif, which becomes exposed under specific conditions, for example in the presence of a lipid bilayer. This topology would place the fusion motif of the opposite end of E2 from the viral membrane, as would be expected in a fusion protein. (*B* and *C*) Activation of E2 by the reduced pH of the endosome and disulfide isomerase activity causes E2 monomers to rotate with respect to each other to a more membrane-perpendicular configuration, promoting membrane insertion of the fusion motif in E1 (*B*), or domain I (*C*). The hydrophobic contacts between aromatic side chains in domain IIIc function as a lubricated hinge. The significant molecular motions require the breakage or isomerization of the disulfide bond at Cys987.